19

The Search for Glacially Induced Faults in Eastern Canada

JOHN ADAMS AND GREGORY R. BROOKS

ABSTRACT

There is abundant evidence of high levels of seismic activity during deglaciation of Eastern Canada, suggesting that the seismic response of Eastern Canada to deglaciation is analogous to Fennoscandia, where numerous glacially induced faults (GIF) have been confirmed. However, the Canadian record of GIFs is scant. The two probable GIFs that are described are few compared to the statistically expected amount of 100+ surface ruptures. Alternative explanations to account for the small number of known ruptures are provided together with an interpretation of certain normal faulting that has been observed in glaciolacustrine sediments. It is recommended that interpretation of prospective GIF features should utilize a sceptical approach employing judgemental scales that reflect data limitations and associated uncertainties.

19.1 Introduction

Eastern Canada (Figure 19.1) represents a large area of glaciated terrain, much of which is underlain by Precambrian Shield bedrock. It was unloaded of 2–3 km of ice mostly between 17,000 and 8,000 years ago (Dyke, 2004), a process marked by an increase in earthquake shaking events immediately after the local deglaciation (Brooks, 2018). Northern Fennoscandia is a much smaller region (about 900,000 km^2) that otherwise appears equivalent in terms of crustal age, crustal thickness, contemporary compressive tectonic stress regime, recent ice load and deglacial process. There, over a dozen deglacial fault scarps have been identified (e.g. Olesen et al., 2004; Lagerbäck & Sundh, 2008; Sutinen et al., 2014; Mikko et al., 2015).

As yet there has been no systematic survey to identify candidate glacially induced faults (GIFs) in Canada. In a recent review, Brooks and Adams (2020) examined GIFs in Eastern Canada that they defined as occurring within an interval of 'several' thousand years after ice-sheet meltback at a given location. For their purposes, Eastern Canada was considered to encompass the Atlantic Canada provinces of Nova Scotia, New Brunswick, Prince Edward Island, Newfoundland and Labrador, the central Canada provinces of Ontario and Quebec, and Manitoba, the easternmost province of Western Canada, an area of about 4 million km^2 (Figure 19.1). They examined the evidence for eleven features from an area

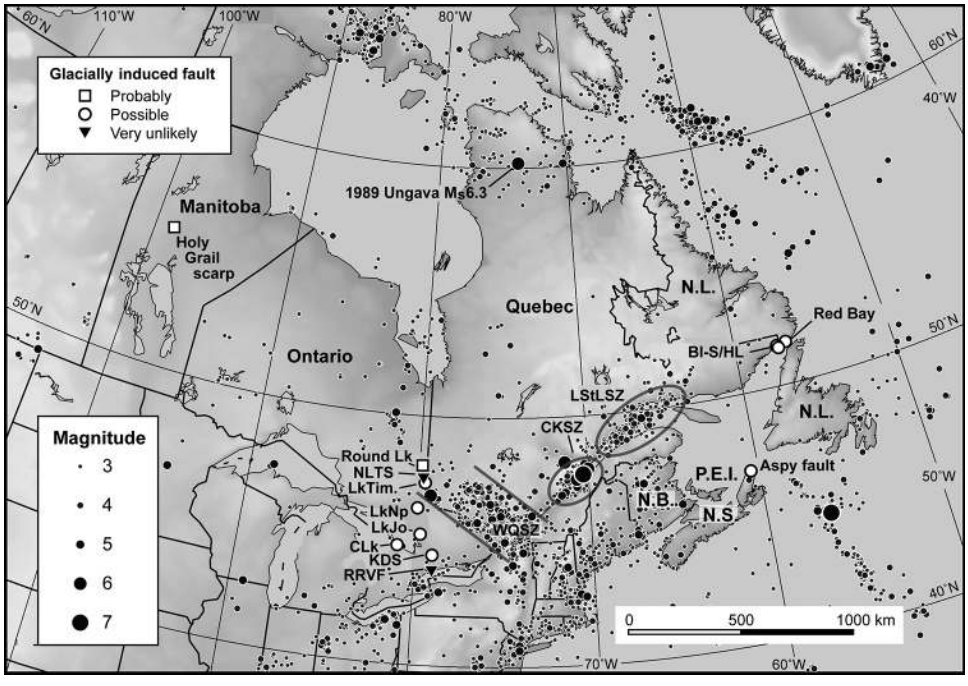

Figure 19.1 Map of Eastern Canada showing the location of historical earthquake epicentres, major seismic zones and the fault features mentioned in the text (modified from Brooks & Adams, 2020). Bl-S/HL – Blanc-Sablon and Hammone Lake; CKSZ – Charlevoix-Kamouraska Seismic Zone; CLk – Charles Lake; LkJo – Lake Joseph; LkNp – Lake Nipissing; LkTim. – Lake Timiskaming; LStLSZ – Lower St. Lawrence Seismic Zone; N.B. – New Brunswick; N.L. – Newfoundland and Labrador; NLTS – New Liskeard-Thornloe scarp; N.S. – Nova Scotia; P.E.I. – Prince Edward Island; RRVF – Rouge River Valley Faults; TESF –Timiskaming East Shore Fault; KDS – Kirkfield deformed shorelines; WQSZ – Western Quebec Seismic Zone (base earthquake map courtesy of the Canadian Hazards Information Service, NRCan).

about four times larger than Fennoscandia and concluded that just the two discussed herein are probable early postglacial GIFs (Figure 19.1; Table 19.1). Neither feature has been documented and confirmed to the degree of the Fennoscandian faults.

This chapter provides context for the occurrence of GIFs in Eastern Canada and reviews briefly the two identified probable examples of GIFs. It discusses the apparent contradiction of observed normal faulting within a region where the contemporary crustal stress conditions produce reverse or strike-slip faulting and provides several alternative explanations to account for the small number of known ruptures.

19.2 Expected Numbers of Glacially Induced Faults

Fennoscandia has been the basis for a model that suggests: (i) seismic strain energy is accumulated during major glaciations because the weight of the ice inhibits reverse faulting

Table 19.1 *Listing of candidate glacially induced faults ranked as 'probable' by Brooks & Adams (2020).*

Location	Latitude/ Longitude	Comments
Holy Grail scarp, Manitoba	55.197° N 99.026° W	Low-angled curvilinear to linear scarp, ~30 km long and 5–8 m high, that forms the east side of a slightly elevated cuesta.
Round Lake, Ontario	48.015° N 80.041° W	A series of faults, some aligned or parallel, with overall ~2-km extent, buried in lake sub-bottom. Faults are normal, 60–545 m long, and offset glaciolacustrine sediments. Offsets are on low-angle fault planes (as low as ~30°) and locally up to several metres. Position and alignment of faults coincides approximately with the mapped Long Lake Fault, which is ~21 km long.

of shield regions; and (ii) the accumulation is released as a burst of large-magnitude earthquakes when the ice load is removed during deglaciation (Johnston, 1987; Adams, 2005; Steffen et al., 2014; Craig et al., 2016). This appears a plausible mechanism for Eastern Canada and is supported by the intense shaking record of early postglacial earthquakes from western Quebec. That record indicates seismicity rates about two orders of magnitude higher than today's rate (Brooks, 2018), even though none of the causative faults have been identified.

Unlike other deglaciated shield regions, Eastern Canada has a documented historical surface rupture, showing that today's crustal stress conditions are favourable for earthquakes to create surface scarps. The 1989 Ungava earthquake (Figure 19.1) was magnitude M_s 6.3, rupturing the top 5–6 km of the crust and forming a 10-km-long fault rupture with a scarp up to 1.3 m high (average height 0.8 m; Adams et al., 1991). Modelling of the surface deformation suggests the rupture occurred on a chiefly reverse fault dipping at 70°, with 1.8 m of slip and with the slip mainly in the top 3 km. Large areas of the Canadian Shield appear to have seismicity confined to the top 5–7 km of crust (Ma et al., 2008), meaning that a significant fraction of their $M > 6$ earthquakes should generate surface ruptures. A statistical analysis (Fenton et al., 2006) suggests that if the historical rates had persisted since deglaciation, 28–160 surface ruptures should have occurred in the Eastern Canada region of Figure 19.1. To these should be added perhaps four times as many from the hypothesized burst of GIFs (by analogy to Sweden; Adams, 2005), for an expected number in the 100–600 range. The additional assumptions to get the factor-of-four increase are that the strain build-up is constant with time, that the last glacial persisted for about four times longer than the time since deglaciation and that the ratio of small to large earthquake numbers (*b*-value) has not changed.

19.3 Probable Glacially Induced Faults

19.3.1 Holy Grail Scarp, Manitoba

The strongest candidate for a GIF in Eastern Canada is the Holy Grail scarp, located in north-central Manitoba about 600 km north of Winnipeg (Figure 19.1). The ~30-km-long

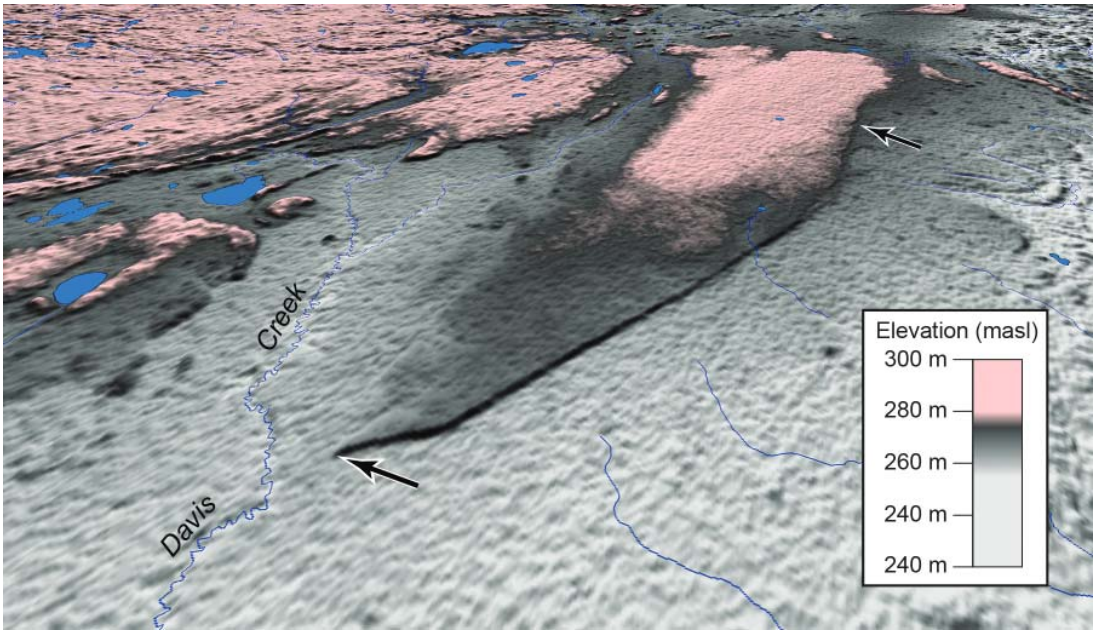

Figure 19.2

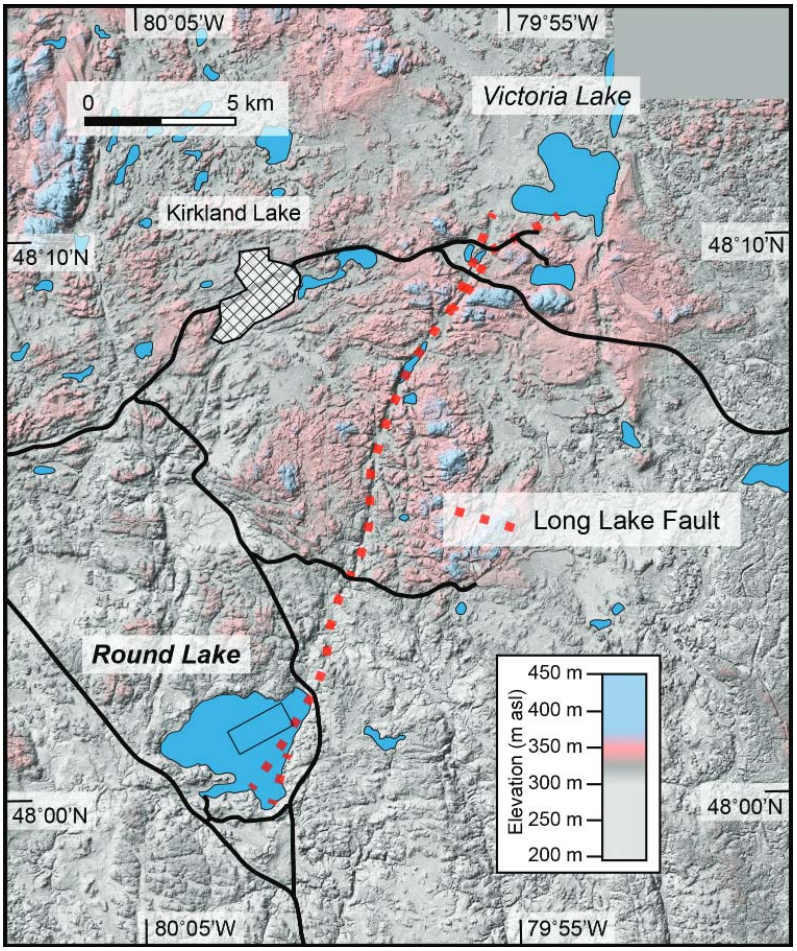

Figure 19.3

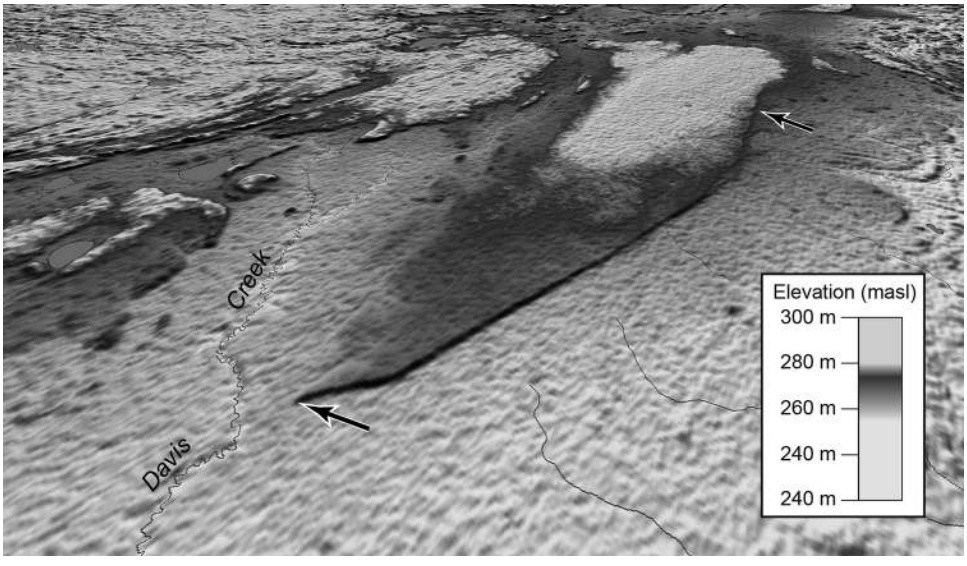

Figure 19.2 Oblique shaded relief digital elevation model (DEM) showing the Holy Grail scarp, north-central Manitoba (see Figure 19.1 for location; V.E. 6X; DEM derived from Shuttle Radar Topography Mission 90 m DEM data courtesy of NASA/JPL-Caltech). Two arrows spaced ~29 km apart mark the extent of the possible fault scarp along the east side of a slightly elevated cuesta. View is approximately northwards. The irregular texture over much of the ground surface probably is an artifact of the low-resolution SRTM DEM. (A black and white version of this figure will appear in some formats. For the colour version, please refer to the plate section.)

scarp is evident on satellite imagery and aerial photographs and forms the east side of a slightly elevated cuesta that is 10–15 m above the surrounding terrain (Figure 19.2). The scarp itself is 5–8 m high, faces east and slopes at less than 5°. Given the low angle of the scarp and the reported geology of the area (see Manitoba Energy and Mines, 1989; McMartin, 1997), the scarp is probably composed of surficial materials.

Remote interpretation of the scarp is complicated because a recessional shoreline of glacial Lake Agassiz was positioned against at least part of the scarp during the Early Holocene (McMartin, 2000; Trommelen, 2014). However, Brooks and Adams (2020) consider it unlikely that the scarp is exclusively the product of shoreline erosion because over its length it has a different longitudinal slope than the shoreline's tilt.

Towards the north, the scarp becomes indistinct. Towards the south, it exhibits a sharp, 26° bend for the last 2 km north of its termination. The feature may extend further to the south of the termination, but the ground surface there is at a lower elevation (light grey in Figure 19.2), and any extension of the rupture may be buried beneath subsequent glacial Lake Agassiz sediments. Burial of a low-level extension by glacial lake deposits is consistent with an early postglacial age for the Holy Grail scarp. Where Davis Creek crosses the possible extension, its channel exhibits changes in course and sinuosity (Figure 19.2; but better shown by Figure 3 of Brooks and Adams, 2020), which may reflect an alteration of the valley slope caused by a buried rupture.

The inferred creek valley slope change and the topographic cuesta are consistent with the scarp caused by slip on a west-dipping thrust fault. With an overall strike of 030 degrees, such a fault would be favourably oriented for reactivation in the generally E-W compressive stress field of Eastern Canada. At a minimum, the length of the sharpest part of the scarp (~15 km) and the scarp height (~5 m) suggest the causative earthquake might have been larger than the Ungava earthquake by a 0.5-magnitude unit (see below), i.e. $M_w = 6.8+$. The Holy Grail scarp is assessed as 'probably' representing a GIF, but trenching or other on-site investigations is required to conclusively establish its earthquake origin.

19.3.2 Round Lake Faulting, Ontario

Based on the preliminary interpretation of sub-bottom acoustic profiling data, Brooks and Adams (2020) reported that under a 1.8 × 0.5-km part of Round Lake are ten short, normal faults that offset just the lower half to two-thirds of the lake's glaciolacustrine deposits. The faults have dips as low as ~30° (Brooks, unpublished data) and have vertical offsets up to several metres. Immediately overlying the faulted sediment is a mass transport deposit, locally up to 2 m thick, that is about 9,100 years old (distinct from, and about 20 varve years older than, the earthquake discussed by Brooks (2020)). The mass transport deposit implies synchronicity for all the fault offsets and (based on experience in other lakes; see Brooks, 2016, 2018) their generation during a shaking event. As the low rigidity of the sediments and the short length of the faults preclude the observed faults being the source of the shaking, the causative earthquake is presumed to have occurred in the underlying Precambrian bedrock.

The occurrence of normal faults like these (similar ones are inferred from profiles in Lake Vättern, for example; see Jakobsson et al., 2014) poses a problem for those studying the seismotectonics of glaciated continents. Firstly, the dominant faulting style for contemporary earthquakes in stable continental regions is reverse or strike-slip faulting – normal faulting mechanisms are unusual. Secondly, there is no strong contender for a normal-faulting GIF, as the Nordmannvikdalen feature in Norway has been now assessed 'very unlikely' to be neotectonic (Redfield & Hermanns, 2016). Brooks and Adams (2020) indicate that the normal faults that offset sediments in Round Lake are not glaciotectonic melt-out structures and that they occurred during the early postglacial period because of their stratigraphic position within the glaciolacustrine deposits of a large glacial lake. The nearby Long Lake Fault, a well-defined bedrock lineament, ~21 km long, extends NNE from the Round Lake area (Figure 19.3) and is an attractive candidate for the causative earthquake rupture, even though there is, as yet, no evidence for postglacial slip on the fault.

How can we reconcile the expected reverse slip on the causative fault with the normal fault offsets of the lake sediments? Below, we suggest a model to link low-dip extensional faulting in deglacial sediments to inferred high-dip reverse faulting in the underlying bedrock; the model might be useful where the bedrock offset has not been imaged.

Consider the effect of a suddenly formed reverse-fault bedrock displacement on a thick overlying sequence of cohesive glaciolacustrine sediments. At its simplest, the originally undeformed horizontal beds extending across the fault would then occur at different

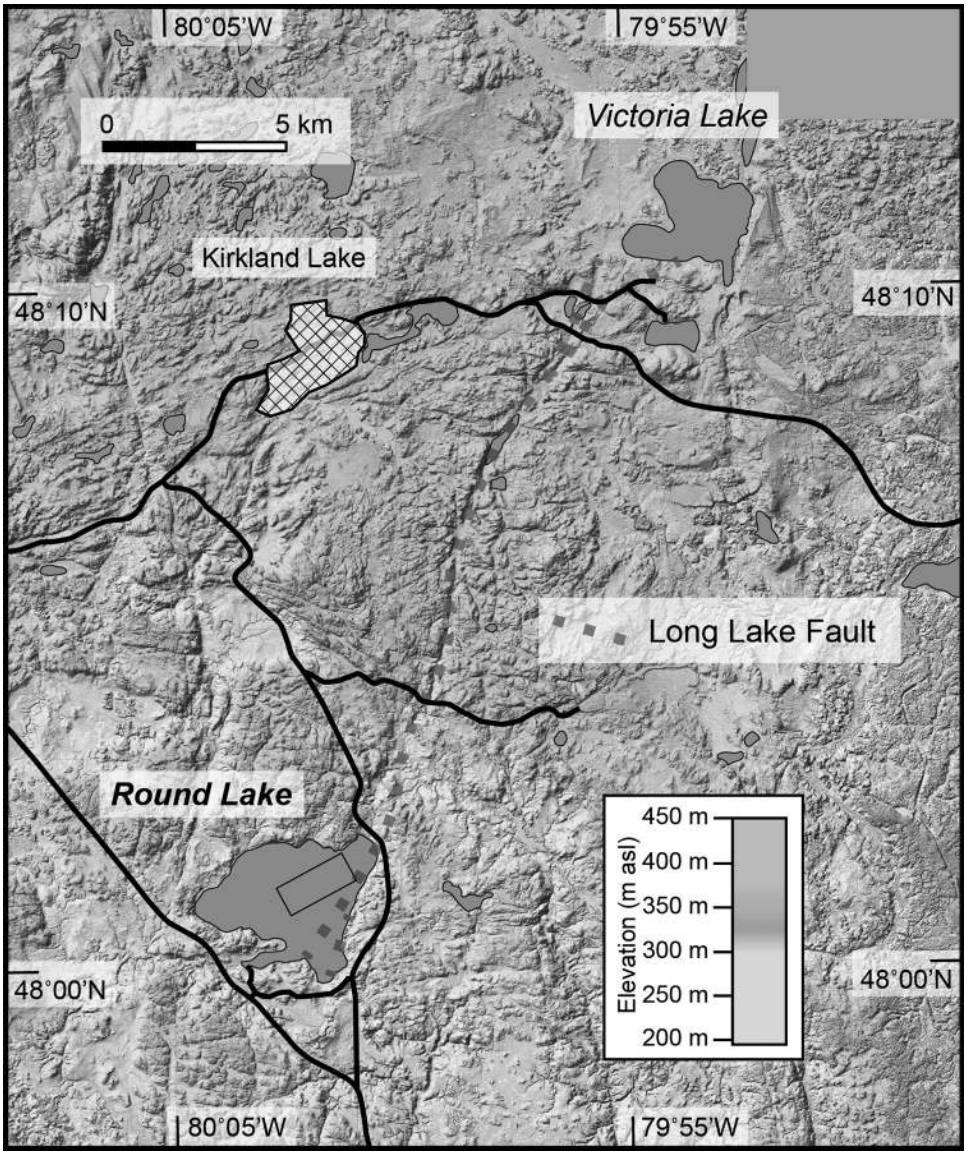

Figure 19.3 Shaded relief map showing Round Lake, the approximate location of the fault features discussed in the text (delineated by a rectangle in Round Lake) and the mapped location of Long Lake Fault and associated bedrock lineament. Location of Long Lake Fault after Ager & Trowell (2000) (V.E. ~6X; shaded relief map derived from a DEM provided by the Ontario Ministry of Natural Resources and Forestry and used under the Open Government License Ontario). (A black and white version of this figure will appear in some formats. For the colour version, please refer to the plate section.)

elevations, established by the uplift on the fault. In some cases, the elevation transition might be modelled as a monoclinal fold with the beds deforming plastically as a trishear (e.g. Erslev, 1991, his Figure 4B). Erslev notes that 'beds adjacent to the anticlinal hinge are commonly thinned and elongated, particularly for higher angle faulting, due to material

flux into the footwall'. However, we observe that some glaciolacustrine sediments behave in a brittle fashion (i.e. macro-faulting of beds in seismic reflection profiles and in subaerial exposures and micro-faulting of rhythmic laminations/beds within core) and so assume in those cases none of the thinning is accommodated by plastic deformation.

As a semi-quantitative example, a prototypical GIF reverse fault with 5 m of throw on a 70° dip causes 1.7 m of shortening of the bedrock and sediments, but 4.7-m uplift on the scarp (Figure 19.4A). The reverse fault, in turn, would cause 4.7-m lengthening to an overlying sediment bed (this assumes the sediment bends closely over the fault scarp), and thus a net 3-m lengthening of the thinned and deformed sedimentary layers across the fault (Figure 19.4B). Steeper bedrock fault dips give even more lengthening, equalling the fault

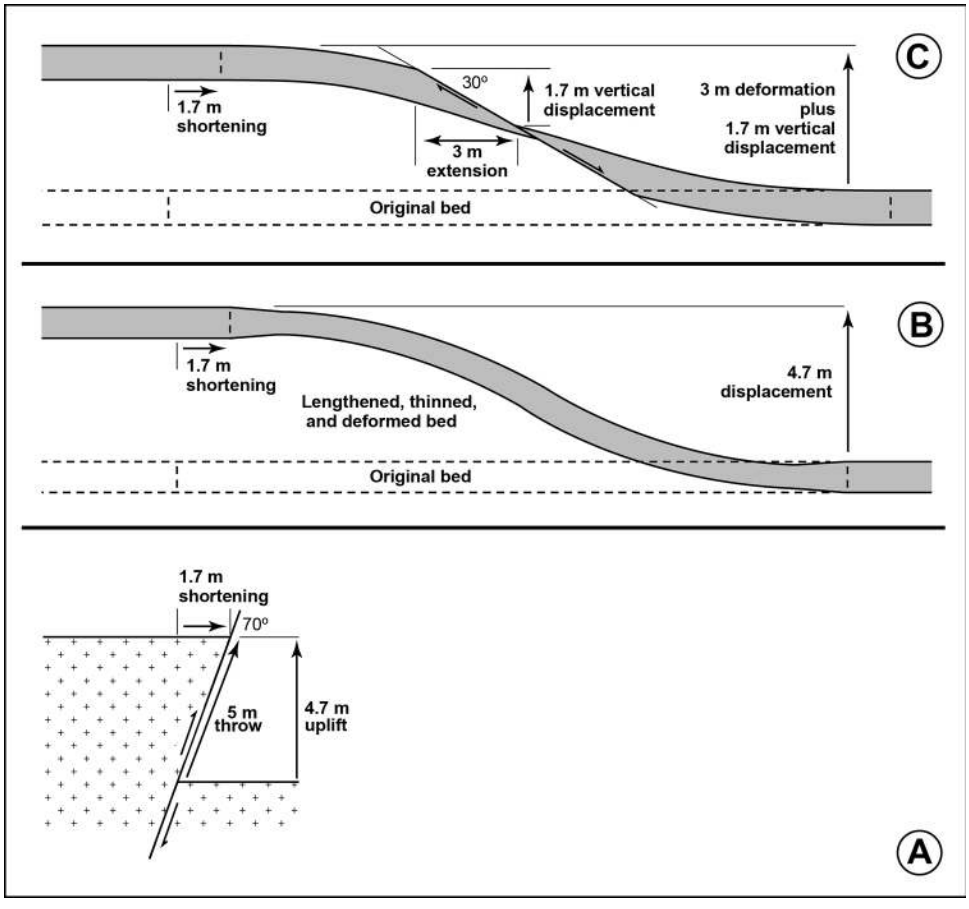

Figure 19.4 Cartoon of example in text (to approximate scale), showing (from bottom) how 5 m of reverse slip on a bedrock fault (A) can cause either (B) plastic bed thinning (deformed bed is 75 per cent of its original thickness) or (C) low-angle normal faulting (as observed at Round Lake) in an overlying sedimentary bed. Both cases would probably not co-exist in a sedimentary sequence above a reverse fault. In this illustration, the footwall is taken as fixed. Thickening of the total sedimentary sequence on the footwall might be expected but is not shown in the figure for clarity.

throw for 90°, while a 45° dip gives no net lengthening. For brittle materials, lengthening is accommodated by extension on normal faults. If the extension takes place on, for example, a 30° dipping normal fault within the sediments (like the Round Lake faults, where we believe we are seeing the true dip), then 3 m of extension could result in about 1.7 m of vertical offset of sedimentary layers (Figure 19.4C). The total extension in the sediments (with corresponding vertical offsets) might be distributed on a number of lesser conjugate normal faults, both synthetic and antithetic, but the sum of the orthogonal extension should relate to the bedrock displacement in the manner above. Furthermore, the normal faults in the sediments should be rooted near the bedrock fault and might dip towards it. 'Near' in this context is within several sediment thicknesses. In this way, a minimum rupture slip (minimum because any horizontal slip component is ignored) might be evaluated from profiles across the fault, then used together with slip-to-magnitude relations to estimate a magnitude for the causative earthquake and hence the likely length of the rupture. Such estimates would provide a basis for reasonableness of the interpretation and could predict the height of exposed bedrock scarps that might be searched for nearby and the distance over which they might be found.

19.4 Other Candidates for Glacially Induced Faults

Brooks and Adams (2020) assessed nine features as 'possible' GIFs (Figure 19.1). The evidence for these is varied: some are probably neotectonic but of the wrong age (Aspy Fault), whereas others are probably the right age but have weak evidence of being neotectonic (sub-aqueous faulting in glaciolacustrine deposits within lakes Timiskaming, Nipissing and Joseph, Ontario; irregularities to the shoreline of a large glacial lake near Kirkfield, Ontario). In addition, there are features with uncertain ages and weak neotectonic evidence (i.e. sinuous ridge feature near Charles Lake, Ontario; examples of reported offset glaciated bedrock surface near Blanc-Sablon and near Hablon Lake, Quebec, and near Red Bay, Newfoundland and Labrador). In every case, more investigation is needed to better evaluate the potential for a GIF origin. In demonstrations of rigorous science, two putative neotectonic faults, the Lower Rouge River Valley faulting and the New Liskeard–Thornloe scarp (Figure 19.1), have been investigated sufficiently to assess them as 'very unlikely' to be GIFs. The former is ascribed to glaciotectonic deformation (ice push; Godin et al., 2002) and the latter is an erosional scarp (Brooks & Pugin, 2019).

19.5 Discussion

The large number of expected surface ruptures (>100) relative to the few known ruptures (the Ungava plus the two probable GIF examples) suggests four possible alternatives.

1. GIFs and surface ruptures never existed in Eastern Canada. However, the region has contemporary earthquakes, with the 1989 Ungava earthquake providing an excellent counterexample of a (late Holocene) surface rupture. Furthermore, the record of early

postglacial earthquake shaking indicates that earthquake activity was widespread and intense during the deglacial period, even if the causative faults have not been identified (Brooks, 2018; Brooks, 2020; Brooks & Adams, 2020). We consider this alternative to be unlikely.

2. GIFs previously existed in Eastern Canada, but almost all scarps formed inside the ice margin and were destroyed by forward movement of the warm-based ice sheet during its last stages of meltback. The erosive nature of the ice was much less in Fennoscandia, which was a cold-based ice sheet, so that any fault scarps formed under its ice could emerge without much modification as the ice melted back. We find the alternative of destroyed scarps unlikely for Canada, as firstly, the large amount of shaking evidence within the postglacial sediments of proglacial lakes in Eastern Canada (see Brooks, 2018; Brooks, 2020; Brooks & Adams, 2020) would only be consistent if the many shaking episodes represented only very large earthquakes far away (so as to be inside the contemporary ice front). For the sequence of earthquakes in the proglacial lakes, this would mean that the required magnitudes would need to be ever larger with time, as the ice front moved ever farther away. Secondly, there are GIFs in Fennoscandia that clearly postdate the ice meltback (e.g. Smith et al., 2014; Sutinen et al., 2014). We recognize that the possibility of preservation through a glacial cycle implies that some Fennoscandian GIFs may be multi-event features and thus more evident in the landscape than a single-event Canadian GIF, but we do not know if this is a contributing factor to the recognition of GIFs there.
3. GIFs still exist but are, and will remain, unrecognized. We note that the long-term discernibility of the Ungava rupture is low because it ruptured through hummocky terrain without clear markers to show offset, extended under lakes for more than half of its length, seldom exposed offset bedrock, and much of its discernibility was due to torn peat and newly exposed lichen-free boulders that will re-vegetate in a few tens to hundreds of years. Even north of the treeline the visual signature is cryptic; in southern Canada widespread tree cover and thick glacial sediment in valleys, lowlands and underlying clay plains additionally reduce the visibility of such faults. We reject this alternative because new data imagery sources, such as Google Earth satellite mosaics with seasonal images, Shuttle Radar Topography Mission DEMs, and LiDAR- and aerial-photograph-derived DEMs, increase the chances that prospective faults will be found. Overall, these new imagery sources – especially bare-earth DEMs – provide good reason to anticipate that additional GIFs will be recognized from a widespread, systematic search for such features.
4. GIFs exist and will be clearly evident once identified. This is the most likely alternative, in our view. However, even if a potential GIF is identified via improved imagery, there are two additional factors that will hinder its confirmation as a GIF. Firstly, GIF study has not been a research priority, meaning that there are few researchers with the skills, experience and resources active in Eastern Canada. Secondly, large areas of northern Quebec, Ontario, Manitoba and Labrador have no road access, thus greatly increasing the cost of the site investigations needed to confirm candidates identified by imagery. As an illustration of both factors, even though the Holy Grail scarp was discovered in the 1970s, there has been no follow-up work.

Although we consider that good potential exists for GIFs in Eastern Canada, we urge an approach that employs scepticism to the interpretation of features as GIFs. Certain topographic features or geological phenomena (examples might be centimetre-scale postglacial faults, superficial stress-release 'pop-ups' in bedrock, river sinuosity changes, sediment drape over drumlins, iceberg furrows, blocky talus along linear features, sackungen and deformed/displaced shorelines attributable to ice remnants) may give a similar appearance to, but lack the continuity and scale expected for, actual fault scarps. The interpretation of a feature as seismogenic (whether glacially induced or otherwise) should be qualified appropriately using a judgement scale that reflects data limitations and associated uncertainties, as was applied by Brooks and Adams (2020). This scale follows Muir Wood (1993) and expresses the interpretation of potential seismogenic faults as 'almost certainly', 'probably', 'possibly', 'probably not' and 'very unlikely' to reflect available information and associated uncertainties. Brooks and Adams (2020) also recognized that the classification of a fault or site-specific evidence of shaking as glacial-induced can be hampered by the feature or event age being poorly constrained. They therefore applied a similar judgement scale for the interpretation of a feature as being glacially induced (i.e. early postglacial in age), applying the terms 'almost certainly', 'probably', 'possibly', 'probably not' and 'very unlikely' as data permit.

19.6 Conclusions

Only two features have been assessed as 'probable' GIFs in Eastern Canada: the Holy Grail scarp, Manitoba, and faulted glaciolacustrine deposits within Round Lake, Ontario. Additional investigation is required to conclusively establish an earthquake origin for the features at both locations. Nine features are considered 'possible' GIFs, but in every case there is much uncertainty about feature age and/or a neotectonic origin.

Additional examples of GIFs should be present in Eastern Canada. The historical background rate of seismicity predicts that 28–160 surface ruptures should have occurred since deglaciation. Perhaps four times as many ruptures can be added to this, arising from the hypothesized burst of seismicity during the early postglacial period.

There is good potential for new prospective GIFs to be identified in Eastern Canada, especially because of the increasing availability of high-resolution, bare earth DEMs. Confirmation that such features are GIFs, however, will be hampered, since GIF study is not a research priority and because of the cost of accessing what is largely remote terrain.

The interpretation of a prospective GIF feature should utilize an approach employing scepticism, qualified appropriately by using judgement scales that reflect data limitations and associated uncertainties.

Acknowledgements

Work on this paper was supported by the Canadian Hazards Information Service and the Public Safety Geoscience Program, Lands and Minerals Sector, Natural Resources Canada.

We thank Dan Clark, Andrée Blais-Stevens and Monica Giona Bucci for their thorough and constructive reviews. This paper represents NRCan Contribution 20190637.

References

Adams, J. (2005). On the probable rate of magnitude $\geq$ 6 earthquakes close to a Swedish site during a glacial cycle. Appendix 5. In S. Hora and J. Mikael, eds., *Expert Panel Elicitation of Seismicity Following Glaciation in Sweden*. Swedish Radiation Protection Authority, No. SSI–2005-20, pp. 33–60.

Adams, J., Wetmiller, R. J., Hasegawa, H. S. and Drysdale, J. (1991). The first surface faulting from a historical intraplate earthquake in North America. *Nature*, **352**, 617–619, doi.org/10.1038/352617a0.

Ager, J. A. and Trowell, N. F. (2000). Geological compilation of the Kirkland Lake area, Abitibi greenstone belt. Ontario Geological Survey, Preliminary Map Series, scale 1:100,000, P3425.

Brooks, G. R. (2016). Evidence of late glacial paleoseismicity from mass transport deposits within Lac Dasserat, northwestern Quebec, Canada. *Quaternary Research*, **86**, 184–199, doi.org/10.1016/j.yqres.2016.06.005.

Brooks, G. R. (2018). Deglacial record of paleoearthquakes interpreted from mass transport deposits at three lakes near Rouyn-Noranda, northwestern Quebec, Canada. *Sedimentology*, **65**, 2439–2467, doi.org/10.1111/sed.12473.

Brooks, G. R. (2020). Evidence of a strong paleoearthquake in ~9.1 ka cal BP interpreted from mass transport deposits, northeastern Ontario – western Quebec, Canada. *Quaternary Science Reviews*, **234**, doi.org/10.1016/j.quascirev.2020.106250.

Brooks, G. R. and Adams, J. (2020). A review of evidence of glacially-induced faulting and seismic shaking in southeastern Canada. *Quaternary Science Reviews*, **228**, doi.org/10.1016/j.quascirev.2019.106070.

Brooks, G. R. and Pugin, A. J.-M. (2019). Assessment of a seismo-neotectonic origin for the New Liskeard–Thornloe scarp, Timiskaming graben, northeastern Ontario. *Canadian Journal of Earth Sciences*, **57**(2), 267–274, doi.org/10.1139/cjes-2019-0036.

Craig, T. J., Calais, E., Fleitout, L., Bollinger, L. and Scotti, O. (2016). Evidence for the release of long-term tectonic strain stored in continental interiors through intraplate earthquakes. *Geophysical Research Letters*, **43**, doi.org/10.1002/2016GL069359.

Dyke, A. S. (2004). An outline of North American deglaciation with emphasis on central and northern Canada. In J. Ehlers and P. L. Gibbard, eds., *Quaternary Glaciations – Extent and Chronology, Part II: North America*. *Developments in Quaternary Science*, Vol. 2, Elsevier, Amsterdam, pp. 373–424, doi.org/10.1016/S1571-0866(04)80209-4.

Erslev, E. A. (1991). Trishear fault-propagation folding. *Geology*, **19**(6), 617–620, doi.org/10.1130/0091-7613(1991)019<0617:TFPF>2.3.CO;2.

Fenton, C. H., Adams, J. and Halchuk, S. (2006). Seismic hazards assessment for radioactive waste disposal sites in regions of low seismic activity. *Geotechnical and Geological Engineering*, **24**, 579–592, doi.org/10.1007/s10706-005-1148-4.

Godin, L., Brown, R. L., Dreimanis, A., Atkinson, G. M. and Armstrong, D. K. (2002). Analysis and reinterpretation of deformation features in the Rouge River valley, Scarborough, Ontario. *Canadian Journal of Earth Sciences*, **39**, 1373–1391, doi.org/10.1139/e02-059.

Jakobsson, M., Björck, S., O'Regan, M. et al.(2014). Major earthquake at the Pleistocene–Holocene transition in Lake Vättern, southern Sweden. *Geology*, **42**, 379–382. Data Repository item 2014142, doi.org/10.1130/G35499.1.

Johnston, A.C. (1987). Suppression of earthquakes by large continental ice sheets. *Nature*, **330**, 467–469, doi.org/10.1038/330467a0.

Lagerbäck, R. and Sundh, M. (2008). *Early Holocene Faulting and Paleoseismicity in Northern Sweden*. Geological Survey of Sweden Research Paper Series C, Volume 836, 80 pp.

Ma, S., Eaton, D. W. and Adams, J. (2008). Intraplate seismicity of a recently deglaciated shield terrane: a case study from Northern Ontario, Canada. *Bulletin of the Seismological Society of America*, **98**, 2828–2848, doi.org/10.1785/0120080134.

Manitoba Energy and Mines (1989). Bedrock Geology Compilation Map Series, preliminary edition, Nelson House, NTS 63-O.

McMartin, I. (1997). Surficial geology, Wuskatasko River area, Manitoba. *Geological Survey of Canada Open File*, **3324**, doi.org/10.4095/208906.

McMartin, I. (2000). Paleogeography of Lake Agassiz and regional post-glacial uplift history of the Flin Flon region, central Manitoba and Saskatchewan. *Journal of Paleolimnology*, **24**, 293–315, doi.org/10.1023/A:1008127123310.

Mikko, H., Smith, C. A., Lund, B., Ask, M. V. S. and Munier, R. (2015). LiDAR-derived inventory of post-glacial fault scarps in Sweden. *GFF*, **137**, 334–338, doi.org/10.1080/11035897.2015.1036360.

Muir Wood, R. (1993). *A Review of Seismotectonics of Sweden*. SKB Technical Report TR 93-13, Stockholm, 243 pp.

Olesen, O., Blikra, L. H., Braathen, A. et al. (2004). Neotectonic deformation in Norway and its implications: a review. *Norwegian Journal of Geology*, **84**, 3–34.

Redfield, T. F. and Hermanns, R. L. (2016). Gravitational slope deformation, not neotectonics: Revisiting the Nordmannvikdalen feature of northern Norway. *Norwegian Journal of Geology*, **96**, 1–29, doi.org/10.17850/njg96-3-05**.**

Smith, C. A., Sundh, M. and Mikko, H. (2014). Surficial geology indicates early Holocene faulting and seismicity, central Sweden. *International Journal of Earth Sciences*, **103**, 1711–1724, doi.org/10.1007/s00531–014-1025-6.

Steffen, R., Wu, P., Steffen, H. and Eaton, D. W. (2014). The effect of earth rheology and ice-sheet size on fault slip and magnitude of postglacial earthquakes. *Earth and Planetary Science Letters*, **388**, 71–80, doi.org/10.1016/j.epsl.2013.11.058.

Sutinen, R., Hyvönen, E., Middleton, M. and Ruskeeniemi, T. (2014). Airborne LiDAR detection of postglacial faults and Pulju moraine in Palojärvi, Finnish Lapland. *Global and Planetary Change*, **115**, 24–32, doi.org/10.1016/j.gloplacha.2014.01.007.

Trommelen, M. S. (2014). Surficial point and line features of the Nelson House map sheet (NTS 63O), Manitoba. Manitoba Mineral Resources, Manitoba Geological Survey Surficial Geology Compilation Map Series SG-GF2013–63O.